Binding of Indanocine to the Colchicine Site on Tubulin Promotes Fluorescence, and Its Binding Parameters Resemble Those of the Colchicine Analogue AC[†]

Lalita Das,[‡] Suvroma Gupta,[‡] Dipak Dasgupta,[§] Asim Poddar,[‡] Mark E. Janik,*[,||] and Bhabatarak Bhattacharyya*[,‡]

Department of Biochemistry, Bose Institute, Kolkata 700054, India, Biophysics Division, Saha Institute of Nuclear Physics, Kolkata 700064, India, and Department of Chemistry, State University of New York, Fredonia, New York 14063

Received August 21, 2008; Revised Manuscript Received November 27, 2008

ABSTRACT: Indanocine, a synthetic indanone, has shown potential antiproliferative activity against several tumor types. It is different from many other microtubule-disrupting drugs, because it displays toxicity toward multidrug resistance cells. We have examined the interaction of indanocine with tubulin and determined their binding and thermodynamic parameters using isothermal titration calorimetry (ITC). Indanocine is weakly fluorescent in aqueous solution, and the binding to tubulin enhances fluorescence with a large blue shift in the emission maxima. Indanocine binds to the colchicine site of tubulin, although it bears no structural similarity with colchicine. Nevertheless, like colchicine analogue AC, indanocine is a flexible molecule in which two halves of the molecule are connected through a single bond. Also, like AC, indanocine binds to the colchicine binding site of tubulin in a reversible manner and the association reaction occurs at a faster rate compared to that of colchicine−tubulin binding. The binding kinetics was studied using stopped-flow fluorescence. The association process follows biphasic kinetics similar to that of the colchicine−tubulin interaction. The activation energy of the reaction was 10.5 ± 0.81 kcal/mol. Further investigation using ITC revealed that the enthalpy of association of indanocine with tubulin is negative and occurs with a negative heat capacity change ($\Delta C_p = -175.1$ cal mol^{-1} K^{-1}). The binding is unique with a simultaneous participation of both hydrophobic and hydrogen bonding forces. Finally, we conclude that even though indanocine possesses no structural similarity with colchicine, it recognizes the colchicine binding site of tubulin and its binding properties resemble those of the colchicine analogue AC.

Tubulin and microtubules are involved in many cellular functions of the life cycle of a eukaryotic cell (*1*). Microtubules are highly dynamic in nature and are composed through rapid polymerization and depolymerization processes. Since anticancer drugs bind either tubulin or microtubules, which modulates the cell cycle, the tubulin−microtubule system has become a very successful target in anticancer drug development. Recent studies suggest that the observed effects of these drugs are due to their interruption of microtubule dynamics rather than the alternation of microtubule polymer mass. This disruption of microtubule dynamics leads to the arrest of cell growth in metaphase and/or anaphase, thereby causing apoptotic cell death or nonapoptotic slow cell death (*2*).

Anticancer drugs have been shown to bind at three major binding sites on tubulin, the vinca, taxane, and colchicine sites (*3*). The taxanes and vinca alkaloids have long been in clinical use; however, these drugs have many drawbacks. The most serious among them is the occurrence of clinical resistance against the drug. Mutations, which include expression of different tubulin isotypes and the overexpression of drug efflux pumps, including the multidrug resistant P-glycoprotein (MDR/Pgp),[1] are responsible for such phenomena. This therefore limits the use of many anti-tubulin agents, and therefore, the search for new drugs or its lead compounds is ongoing. Moreover, most drugs (e.g., paclitaxel) in clinical use require intravenous injection with long-term remedial course, causing patients to suffer mentally and physically and thereby reducing the patients' quality of life. While taxanes are effective against ovarian, lung, breast, bladder, and hematological cancers (*4*), they are ineffective against solid tumors like gastric, liver, and colorectal carcinomas. Therefore, at present, efforts aimed at developing new anti-tubulin drugs that are less vulnerable to resistance, can be administered orally, have broad-spectrum efficiency, and cause minimal neurotoxicity continue (*5*−*10*).

Indanocine (Figure 1) is a potent microtubule-depolymerizing agent with antiproliferative activity (*11*). It induces apoptotic cell death in a broad range of human tumor cell lines, including several types of multidrug resistant cells (*11*). It is different from many other microtubule-disrupting drugs

[†] The financial support from CSIR, India, is gratefully acknowledged.

* To whom correspondence should be addressed. B.B.: Department of Biochemistry, Bose Institute, Centenary Campus, P-1/12, CIT Scheme VII M, Kolkata 700054, India; fax, 91-33-2355-3886; telephone, 91-33-2355-0256; e-mail, bablu@boseinst.ernet.in.

[‡] Bose Institute.

[§] Saha Institute of Nuclear Physics.

[||] State University of New York.

[1] Abbreviations: AC, 2-methoxy-5-(2′,3′,4′-trimethoxyphenyl)tropone; CSI, colchicine site inhibitor; GTA, ethylene glycol bis(β-aminoethyl ether)-*N*,*N*,*N*′,*N*′-tetraacetic acid; GTP, guanosine 5′-triphosphate; ITC, isothermal titration calorimetry; MDR, multidrug resistance; Me_2SO, dimethyl sulfoxide; $MgCl_2$, magnesium chloride; Pgp, P-glycoprotein; PIPES, piperazine-*N*,*N*′-bis(2-ethanesulfonic acid); SAR, structure−activity relationship.

10.1021/bi801575e CCC: $40.75 © 2009 American Chemical Society
Published on Web 01/30/2009

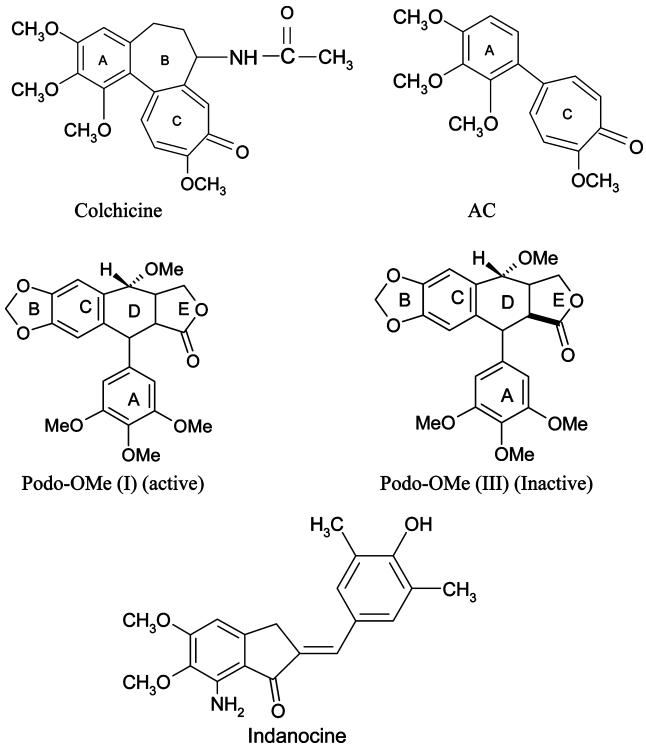

FIGURE 1: Structure of drugs. Colchicine, 2-methoxy-5-(2′,3′,4′-trimethoxyphenyl)tropone (AC), the 4′-methoxy analogue of podophyllotoxin I (active compound) and III (inactive compound), and indanocine are shown.

because it displays toxicity toward multidrug resistant cells and kills nondividing or quiescent cells (*11*). From the literature, it is known that indanocine is potently cytotoxic to several tumor and different MDR cell lines. This sensitivity to MDR cancer cells suggest that indanocine in the near future may be considered as a potential lead compound for the development of anticancer drug.

Although appreciable advancement in the potency of the indanocine has been confirmed at cellular levels, its binding properties with tubulin have remained unexplored. It is therefore important that we know where exactly this drug binds to tubulin, its binding characteristics, its binding thermodynamics, and identification of pharmacophoric attachment point to make improved analogues in the future. Nguyen et al. identified pharmacophoric attachment points for a number of colchicine site inhibitors (CSIs) with diverse structures, including indanocine using molecular dynamics and docking studies (*12*). As indanocine possesses no structural resemblance with colchicine, we are curious to know whether the binding property of the compound is consistent with colchicine during binding to tubulin. In this paper, for the first time, we explore the mode of interaction, along with the kinetic and thermodynamic properties of this promising drug with tubulin.

MATERIALS AND METHODS

Materials. PIPES, EGTA, GTP, colchicine, and podophyllotoxin were purchased from Sigma Chemical Co. Indanocine (catalog no. 402080, lot no. B35514) was purchased from CalBiochem. All *n*-alcohols were spectroscopic grade and purchased from Spectrochem. All other reagents were of analytical grade.

Drugs. A stock solution of indanocine was made with 100% DMSO.

Tubulin Isolation and Estimation. Tubulin was isolated from goat brain by two cycles of temperature-dependent assembly and disassembly in PEM buffer [50 mM PIPES, 1 mM EGTA, and 0.5 mM $MgCl_2$ (pH 6.9)], in the presence of 0.1 mM GTP, followed by two additional cycles in 1 M glutamate buffer (*13*). The purified tubulin, free of MAPs, was stored in aliquots at −70 °C. Protein concentrations were estimated by the method of Lowry et al. (*14*), using bovine serum albumin as the standard. Tubulin preparations used in this study contained a natural mixture of isoforms (*15*). Both calorimetry and fluorescence measurements were carried out with this unfractionated tubulin, and therefore, the binding parameters obtained here are averages for the different isoforms.

Tubulin Polymerization Assay. Pure tubulin in PEM [50 mM PIPES (pH 6.9), 1 mM EGTA, and 0.5 mM $MgCl_2$] buffer was polymerized at 37 °C in the presence of 1 mM GTP. Polymerization was initiated using 10% dimethyl sulfoxide (Me_2SO), and the turbidity was measured by the absorbance at 410 nm rather than at the usual 360 nm (as indanocine has absorption maxima near 360 nm). A Shimadzu UV-160 double-beam spectrophotometer, fitted with a temperature-controlled circulating water bath accurate to ±0.2 °C, was used for this purpose. IC_{50} values were calculated using the concentration of the drug that caused 50% inhibition of polymer mass.

Binding Measurements by the Fluorescence Method. The binding of the ligands to the protein was monitored by enhancement of ligand fluorescence in the presence of protein. Fluorescence spectra were recorded using a Hitachi F-3000 fluorescence spectrophotometer connected to a constant-temperature circulating water bath accurate to ±0.2 °C. All fluorescence measurements were carried out in a 0.5 cm path length quartz cuvette. Excitation and emission wavelengths used for the measurement were 360 and 500 nm, respectively. In all cases, the excitation and emission band-passes were 10 and 5 nm, respectively. Fluorescence values were corrected for the inner filter effect using the Lakowicz equation (*16*) $F_{cor} = F_{obs}[\text{anti log}(A_{ex} + A_{em})/2]$, where A_{ex} and A_{em} are the absorbance at the excitation and emission wavelengths, respectively.

A modified Dixon plot of indanocine was obtained using podophyllotoxin as a competitive inhibitor. The reaction mixtures containing tubulin (3 μM), varied concentrations of indanocine (5−15 μM), and podophyllotoxin (0−40 μM) were incubated at 37 °C for 20 min. The reciprocal of the fluorescence intensity of the indanocine−tubulin complex at 500 nm was plotted against the concentration of podophyllotoxin.

Measurement of Kinetics and Activation Energy. The kinetics of the association of indanocine with tubulin was measured under pseudo-first-order conditions using stopped-flow fluorescence measurement. The fast kinetics was studied using a SFA-20 rapid kinetic accessory from Hi-Tech Scientific attached to a Perkin-Elmer LS-55 luminescence spectrofluorimeter. The dead time of the instrument was found to be 20 ms. The temperature was controlled with a circulating water bath accurate to ±0.2 °C.

For experiments monitoring the quenching of tryptophan fluorescence, samples were excited at 280 nm and the

emission intensities were recorded at 335 nm. The excitation and emission band-passes were 5 nm each. The quenching data were analyzed in the same way as the ligand fluorescence data, using the following biexponential equation:

$$F = Ae^{-k_f t} + Be^{-k_s t} \quad (1)$$

where F is the fluorescence of the ligand−tubulin complex at time t, A and B are the amplitudes for the fast and slow phases, respectively, and k_f and k_s are the pseudo-first-order rate constants for the respective phases. The observed rate constants (k_{obs}) were determined under pseudo-first-order conditions where the indanocine concentration varied from 10 to 40 μM and the tubulin concentration was kept at 1 μM.

For monitoring of drug fluorescence, an excitation wavelength of 360 nm and an emission wavelength of 500 nm were used. The excitation and the emission band-passes were 5 nm each. The kinetics was corrected for free drug fluorescence by measuring the fluorescence after mixing of an appropriate concentration of indanocine in PEM buffer.

The data of increasing ligand fluorescence as a function of time were fit to the equation (*17*)

$$F_\infty - F = Ae^{-k_f t} + Be^{-k_s t} \quad (2)$$

where F_∞ is the maximum fluorescence intensity corresponding to six half-lives of the reaction, F is the fluorescence intensity at time t, k_f and k_s are the observed rate constants of the fast and slow phases, respectively, and A and B are the amplitudes of these two phases. The parameters A, B, C, k_f, and k_s were obtained by nonlinear curve fitting using Microcal Origin 7.5.

The observed rate constant (k_{obs}) was determined at different temperatures ranging from 15 to 42 °C, and the activation energy (E_a) was calculated by plotting ln k_{obs} versus $1/T$ according to the Arrhenious equation [$k_{obs} = A \exp(-E_a/RT)$, where A is the pre-exponential factor].

Calorimetry. Isothermal titration calorimetric measurements were performed on a VP-ITC MicroCalorimeter from MicroCal, Inc. (Northampton, MA). Tubulin (10−12 μM) was dialyzed extensively against PEM buffer with 0.1 mM GDP (to offer stabilization), and indanocine (130 μM) was dissolved in the last dializant. The pH values of the tubulin and the ligand solutions were made identical before they were loaded into the calorimeter. A typical titration involved 25 injections of ligand (10 μL aliquots/shot), at 3 min intervals, into the sample cell (volume of 1.4359 mL) containing tubulin. The titration cell was kept at a definite temperature and stirred continuously at 310 rpm. The heat of dilution of the ligand in the buffer alone was subtracted from the titration data. Data acquisition and analysis were performed using inbuilt Microcal Origin 5.0 to determine the binding stoichiometry (N) and thermodynamic parameters of the reaction. The "One Set of Sites" binding model, provided with the software, was used. Enthalpy changes (ΔH) and affinity constants (K_a) were known after the curve fitting. The changes in free energy (ΔG) and entropy (ΔS) were calculated using the following equations:

$$\Delta G = \Delta G^\circ + RT \ln K_a \text{ (at equilibrium, } \Delta G^\circ = 0) \quad (3)$$

$$\Delta G = \Delta H - T\Delta S \quad (4)$$

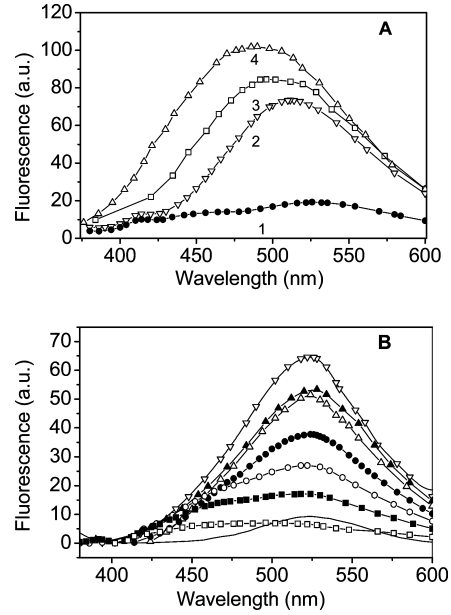

FIGURE 2: (A) Fluorescence emission spectra of indanocine (20 μM) in buffer (curve 1) and 5 μM indanocine complexed with 5 (curve 2), 10 (curve 3), and 25 μM (curve 4) tubulin at 37 °C. The excitation and emission wavelengths were 360 and 500 nm, respectively. (B) Fluorescence emission spectra of indanocine (15 μM) in water (—), methanol (□), ethanol (■), propanol (○), butanol (●), hexanol (△), octanol (▲), and decanol (▽). The excitation wavelength was the same as in panel A.

The thermodynamic parameters ΔG, ΔH, and ΔS were determined over a range of temperatures from 20 to 37 °C. Therefore, the heat capacity change at constant pressure (ΔC_p) was determined using Kirchoff's equation as

$$d\Delta H/dT = \Delta C_p \quad (5)$$

A plot of the enthalpy change (ΔH) of indanocine−tubulin binding as a function of temperature yields ΔC_p.

RESULTS

Promotion of Indanocine Fluorescence upon Binding to Tubulin. Preliminary spectroscopic studies indicate that indanocine is weakly fluorescent in aqueous solution. Binding to tubulin enhances fluorescence intensity and shows a large blue shift in the emission maxima with an increase in the concentration of protein [λ_{max} shifted from 530 nm (in free drug) to 487 nm (in complex)]. This enhancement of fluorescence intensity along with the shifting of λ_{max} of indanocine with addition of an increasing concentration of tubulin at 37 °C is shown in Figure 2A.

Indanocine, by virtue of its several aromatic rings, may act as a nonspecific hydrophobic fluorophore, thereby binding to hydrophobic patches of proteins and promoting fluorescence. Therefore, we tested indanocine binding with several proteins such as bovine serum albumin, α-lactalbumin, ovalbumin, lactate dehydrogenase, and carbonic anhydrase. Indanocine did not fluoresce in the presence of these proteins, indicating the specificity of indanocine binding to tubulin (Table 1).

In this context, it should be mentioned that there is only one antimitotic drug known which exhibits similar properties upon binding to tubulin. This is the most studied antimitotic drug, colchicine, that is nonfluorescent in aqueous solution

Table 1: Fluorescence of Indanocine with Different Proteins[a]

protein (30 μM in all cases)	fluorescence after binding (arbitrary units)
tubulin	100[b]
bovine serum albumin	~4
α-lactalbumin	<4
ovalbumin	<3
lactate dehydrogenase	~6
carbonic anhydrase	<6

[a] The indanocine concentration was 3 μM in all cases. The drug−protein complex was prepared in PEM buffer and incubated at 37 °C for 15 min. Fluorescence was measured upon excitation at 360 nm. [b] The fluorescence intensity in presence of 30 μM tubulin was normalized to 100 for easy comparison of the results with those of other proteins.

but shows intense fluorescence upon binding to tubulin (*18*). Both indanocine and colchicine exhibit fluorescence upon binding to tubulin, although they bear no structural similarity to each other. Enhancement of fluorescence on binding of a small ligand to a protein is generally explained as arising due to the hydrophobic environment provided by the binging site, thus lowering the probability of mobile dipole-dependent internal conversion processes. The fact that solvents of low polarity also facilitate such fluorescence enhancement is used as a support for their mechanism. Therefore, the fluorescence of indanocine in a series of *n*-alcohols was measured as shown in Figure 2B. The fluorescence increased significantly when the solvent was changed from methanol to *n*-octanol; however, there was no significant blue shift in the observed emission maxima. In this study, the binding of tubulin to indanocine not only enhanced the fluorescence intensity of the drug but also showed a large blue shift in the emission maxima with an increase in the concentration of the protein. It is an established fact that a molecule that exhibits a large excited-state dipole renders its emission spectrum quite sensitive to the relaxation of the solvents. For example, prodan shows a large blue shift in its emission maxima in the presence of proteins due to the reorientation of the solvent molecules around the excited-state dipole (*19*). More studies are required to establish whether a similar mechanism is also responsible for the observed blue shift in indanocine fluorescence upon tubulin binding.

Indanocine Binds Reversibly at the Colchicine Site of Tubulin. Indanocine has no structural resemblance with colchicine or podophyllotoxin. However, it was reported that indanocine competes with [^{3}H]colchicine for its binding to tubulin (*11*). Podophyllotoxin also competes for the colchicine binding site of tubulin which has been ascribed to the fact that both possess a trimethoxyphenyl ring (ring A, Figure 1). To determine whether indanocine binds at the colchicine site of tubulin, indanocine was allowed to compete with podophyllotoxin for binding to tubulin, and the data were analyzed using a modified Dixon plot (Figure 3A). The binding was studied fluorometrically using indanocine fluorescence. The results presented in Figure 3A clearly indicate that podophyllotoxin inhibited competitively binding of indanocine to tubulin with a K_i value of ~13.5 μM. Results of a modified Dixon plot established that indanocine also binds to the colchicine site of tubulin. Another important property of colchicine−tubulin interaction is its irreversibility. While a structurally flexible colchicine analogue like AC and podophyllotoxin bind to tubulin with a faster on rate, the off rates of binding of colchicine and its analogues

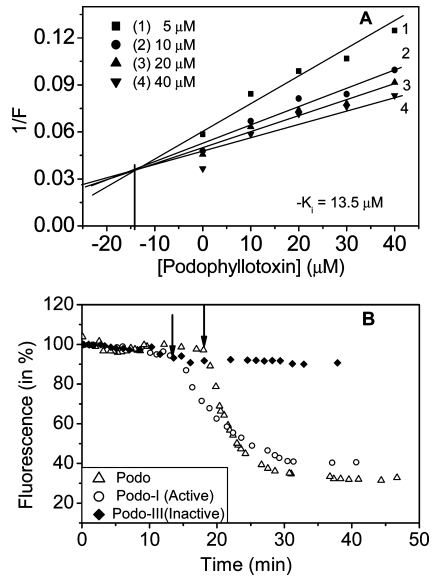

FIGURE 3: (A) Modified Dixon plot. The reaction mixtures contained 3 μM tubulin, indanocine, and podophyllotoxin at the indicated concentrations and were incubated at 37 °C for 20 min. Excitation and emission wavelengths were 360 and 500 nm, respectively. (B) Binding of indanocine (5 μM) to tubulin (5 μM). In both cases, after saturation, 100 μM podophyllotoxin-OMe(III) (inactive) and 100 μM podophyllotoxin-OMe(I) (active) were added and binding was monitored fluorometrically. The arrows in the curve indicate the time when podophyllotoxin analogues were added to the reaction mixture.

are related to both the B-ring and its side chain at the C-7 position (*20, 21*). We are, therefore, curious to know whether indanocine binding to tubulin is reversible like the AC−tubulin interaction as both AC and indanocine are structurally flexible, where two halves of the molecule can act as a bifunctional ligand.

We measured the reversibility of indanocine binding to tubulin using podophyllotoxin and a 4′-methoxy derivative of podophyllotoxin (Figure 3B). This particular 4′-methoxy position of the oxalone ring of podophyllotoxin is important for the recognition of the binding site as its stereoisomer, 4′-methoxy derivative of podophyllotoxin is inactive [Podo-OMe(III)] (Figure 1). Similarly, introduction of a sugar group at the 4′-methoxy position makes an inactive compound, etoposite (*22*). Therefore, the purpose of using these two 4′-methoxy isomers of podophyllotoxin for this experiment was to test the specificity of indanocine in recognizing the binding site of podophyllotoxin. For this experiment, the indanocine−tubulin complex was prepared by mixing 5 μM tubulin and 5 μM indanocine at 37 °C. The complex was divided into different test tubes for testing with these analogues of podophyllotoxin. Experiments were performed upon measurement of the indanocine fluorescence in the presence of podophyllotoxin derivatives. Results of such experiments are shown in Figure 3B. As shown in this figure, the addition of 100 μM podophyllotoxin or the active 4′-methoxy derivative of podophyllotoxin [Podo-OMe(I)] to the complex causes a roughly identical decrease in the initial fluorescence of indanocine (60−65%), whereas 100 μM inactive analogue [Podo-OMe(III)] has no effect on indanocine−tubulin fluorescence (Figure 3B). These results indicate that the indanocine reversibly binds to the colchicine binding site and recognizes all important points of attachment of active podophyllotoxin to the colchicine site of tubulin.

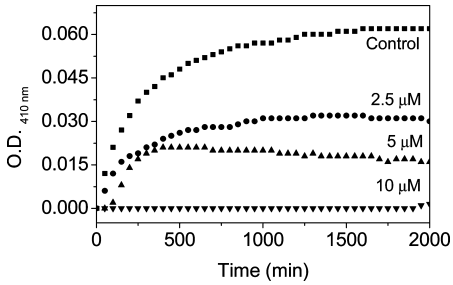

FIGURE 4: Effect of indanocine on tubulin polymerization. Tubulin (15 μM) was mixed with indanocine at different concentrations as follows: 0 (■), 2.5 (●), 5 (▲), and 10 μM (▼) at 37 °C in PEM buffer. Polymerization was recorded for 2000 s. Polymerization was initiated by the addition of 10% dimethyl sulfoxide (Me_2SO) followed by the addition of 1 mM GTP.

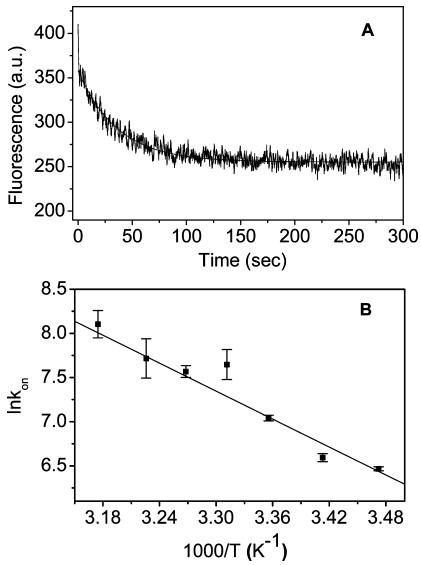

FIGURE 5: (A) Indanocine binding to tubulin using stopped-flow analysis. The best-fit line to the fluorescence decrease for the binding of indanocine and tubulin at 25 °C is shown. The rate constant of this compound was measured by mixing tubulin (1 μM) with indanocine (10 μM), and the decrease in fluorescence was recorded with time. Samples were excited at 280 nm, and emission was measured at 335 nm. (B) Effect of temperature on the association rate constant of indanocine binding to tubulin. Details of the experiment are given in Materials and Methods.

Inhibition of Tubulin Polymerization by Indanocine. We tested the inhibition of tubulin polymerization upon indanocine binding using dimethyl sulfoxide (Me_2SO). In vitro, indanocine shows progressive concentration-dependent inhibition of tubulin self-assembly with an IC_{50} of 2.85 μM (Figure 4). Under identical conditions, colchicine inhibited tubulin self-assembly with an IC_{50} of ~6.5 μM.

Stopped-Flow Fluorescence Kinetic Study. The kinetics of the indanocine−tubulin association reaction was studied monitoring the quenching of intrinsic protein fluorescence under pseudo-first-order condition, with indanocine present in an at least 10-fold molar excess. The tubulin fluorescence emission at 335 nm (with excitation at 280 nm) was quenched with time. A representative kinetic profile is shown in Figure 5A. The rate constant was obtained by fitting the data to a biexponential function. The apparent second-order rate constant values are nearly $(6.81 \pm 1.2) \times 10^3$ M^{-1} s^{-1} for the major fast phase and $(1.42 \pm 0.6) \times 10^3$ M^{-1} s^{-1} for the minor slow phase at 25 °C. The value obtained in the case of a fast phase is ~10 times slower than that of AC

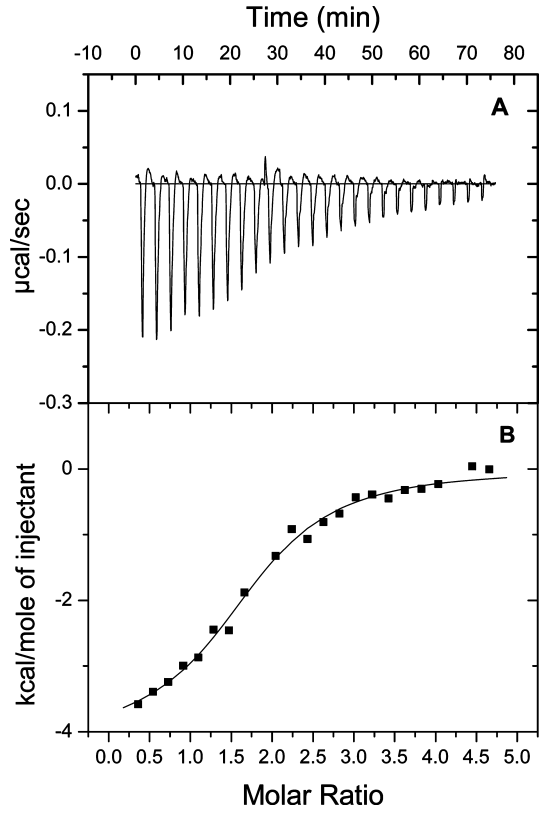

FIGURE 6: Calorimetric titration of tubulin with indanocine. (A) Raw data obtained from 25 injections (10 μL each) of indanocine (130 μM) into 11 μM tubulin in 50 mM PEM buffer (pH 7). (B) Nonlinear least-squares fit of the incremental heat per mole of added ligand for the titration in panel A as a function of the molar ratio use Origin 5.0.

binding to the tubulin (*21*). The apparent second-order rate constant may be calculated according to $k_{obs} = k_{app}$[indanocine].

To measure the activation energy of indanocine−tubulin interaction, the rate constant of the fast phase was measured over a temperature range of 15−42 °C at a fixed indanocine concentration (20 μM) and a fixed tubulin concentration (1 μM). Figure 5B shows these data as an Arrhenius plot, from which activation energy of 10.5 ± 0.81 kcal/mol was obtained for the association reaction of indanocine−tubulin binding. Reported values of the activation energy for colchicine and AC−tubulin binding were 20.4 ± 0.3 and 13.0 ± 1.0 kcal/mol, respectively (*21, 23*).

Thermodynamic Parameters Using Isothermal Titration Calorimetry. Thermodynamic parameters such as the Gibbs free energy change (ΔG), enthalpy change (ΔH), and entropy change (ΔS) along with the number of binding sites (N) and affinity constant (K_a) can provide useful information for identifying fundamental forces involved in protein−drug interaction. Moreover, determination of binding enthalpy as a function of temperature yields changes in heat capacity, which is associated with an interaction that provides a valuable insight into the type of forces involved therein. Thus, to decipher the nature of interaction of indanocine with tubulin, the thermodynamics of binding of indanocine with tubulin was performed using isothermal titration calorimetry (ITC). Figure 6A shows the raw data of a calorimetric experiment, which involved the titration of tubulin with indanocine in PEM buffer at 30 °C. As is evident from the figure, the binding reaction is characterized by a significant

Table 2: Thermodynamic Parameters of Indanocine−Tubulin Interactions

temp (K)	ΔH (cal/mol)	ΔS (cal mol^{-1} K^{-1})	$T\Delta S$ (cal/mol)	ΔG (cal/mol)	ΔC_p (cal mol^{-1} K^{-1})
293	−1381 ± 80.4	20.76	6082.68	−7463.68	−175.1
298	−2558 ± 100.1	16.35	4872.30	−7430.30	
306	−3632 ± 128.8	13.18	4033.08	−7665.08	
310	−4507 ± 543.7	8.165	2531.15	−7038.15	

heat change. The drug exhibits a stoichiometry of 1 for binding to tubulin. Figure 6B represents the enthalpy change upon binding for each injection as a function of the concentration of indanocine for each injection. The thermodynamic parameters ΔG, ΔH, and ΔS are determined over a range of temperatures from 20 to 33 °C and are presented in Table 2. The affinity constant of the binding is 2.8×10^5 M^{-1} at 25 °C.

Here both ΔH and ΔS exhibited clear temperature dependence (Table 2). The free energy of binding (ΔG) did not vary greatly with temperature, but ΔS varied in a compensatory manner with ΔH. Enthalpy−entropy compensation is associated with solvent reorganization accompanying protein−ligand interactions (*24, 25*). A linear relationship of ΔH with $T\Delta S$ with a slope exactly equal to 1 is an indication of complete compensation. Figure 7A shows an enthalpy−entropy compensation plot depicting the variation of ΔH as a function of $T\Delta S$. The slope $d\Delta H/d(T\Delta S)$ was equal to 0.895. Therefore, we observed partial enthalpy−entropy compensation for drug binding. Such a compensatory effect is well-known for protein−ligand binding (*26*).

The heat capacity change at constant pressure (ΔC_p) is determined using Kirchoff's equation as $\Delta C_p = d\Delta H/dT$. A plot of the enthalpy change (ΔH) of indanocine−tubulin binding as a function of temperature yields a ΔC_p of −175.1 cal mol^{-1} K^{-1} (Figure 7B). This value of ΔC_p for indanocine−tubulin interaction lies in between the values of ΔC_p reported for AC−tubulin and podophyllotoxin−tubulin interaction [$\Delta C_{p(\text{podo})} = -590.3$ cal mol^{-1} K^{-1}, and $\Delta C_{p(\text{AC})} = -69.3$ cal mol^{-1} K^{-1}] (*22*). The significantly lower ΔC_p value observed for AC binding indicates a smaller extent of surface−surface association between the protein−drug interfaces and the predominant involvement of hydrogen bonding during the reaction.

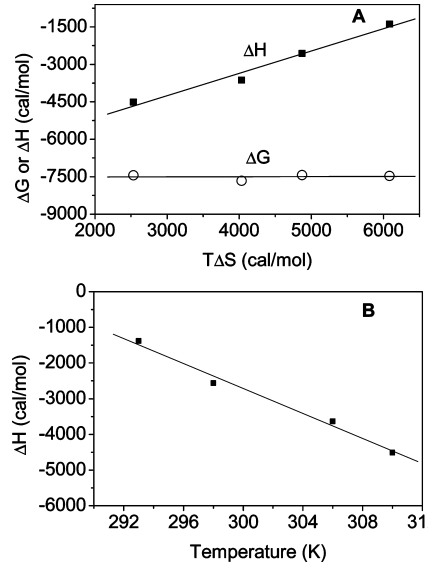

FIGURE 7: (A) Enthalpy−entropy compensation plot for the binding of indanocine to tubulin. Dependence of ΔG (○) and ΔH (■) as a function of $T\Delta S$. (B) Temperature dependence of the enthalpy change (ΔH) of the indanocine−tubulin interaction as a function of T.

DISCUSSION

Indanocine, a synthetic antimitotic indanone, possesses unique properties for functioning as an ideal chemotherapeutic agent as it selectively kills malignant B cells at doses that do not affect normal B cells (*11*). Indanocine is cytotoxic to multidrug resistant cancer cells at the G2/M boundary and induces apoptotic cell death (*11*). It interacts with tubulin at the colchicine binding site, potently inhibiting microtubule polymerization (*11*). While many properties of indanocine at the cellular level are reported, its binding with purified target protein tubulin has not yet been reported.

Fluorescence spectroscopy is a powerful tool for studying ligand−protein interactions. We observed that indanocine which fluoresces very poorly in aqueous solution shows intense fluorescence in the presence of tubulin. Like AC, binding of indanocine to tubulin is instantaneous at room temperature. Indanocine not only shows higher emission intensity in the presence of tubulin but also shows a significant blue shift of the drug emission maxima. It is commonplace in the interpretation of protein binding-induced enhancement of small ligands to ascribe these effects to the hydrophobic nature of the binding site because similar effects can be seen in nonpolar solvents. We have tested indanocine fluorescence in *n*-alcohol series starting from methanol to octanol. While a significant increase in emission intensity is observed in higher alcohols, there is no significant shift in emission λ_{max}.

A number of examples exist in the literature that suggest that immobilization-induced enhancement of fluorescence resulting from protein binding may be more prevalent than generally imagined (*27, 28*). Indanocine is a flexible molecule in which two halves of the molecules are connected through a single bond. Therefore, the binding of indanocine to tubulin will immobilize the flexible drug molecule at the binding site. This structural flexibility of indanocine is comparable with that of AC, a colchicine analogue which shows no detectable fluorescence in aqueous solution. Like indanocine, AC also shows enhanced fluorescence intensity in normal alcohol series but no shift in emission λ_{max}. Most significant differences in their binding properties are large blue shifts in emission λ_{max} of indanocine fluorescence when titrated with tubulin, while there is no significant shift detected when AC is titrated with tubulin under identical conditions. It is known that the shifts in emission λ_{max} are due to molecular motion; i.e., reorientation of the solvent molecules around the excited-state dipole and prodan is a classic example of such a phenomenon (*19*). Whether such a phenomenon is also operating here needs further work on the mechanism of observed fluorescence.

Because of the greater sensitivity of the quenching signal, the kinetics of the indanocine−tubulin association reaction was studied by monitoring tryptophan fluorescence under pseudo-first-order conditions, and the best fit was obtained with a biexponential function. The apparent second-order

Table 3: Hydrophobic and Vibrational Contributions to ΔC_p and ΔS for Indanocine−Tubulin Binding

temp (K)	$\Delta C_{p(\text{hydro})}$[a] (cal mol^{-1} K^{-1})	$\Delta C_{p(\text{vib})}$ (cal mol^{-1} K^{-1})	$\Delta S_{(\text{hydro})}$ (cal mol^{-1} K^{-1})	$\Delta S_{(\text{vib})}$ (cal mol^{-1} K^{-1})
293	−156.163	−18.897	40.602	−19.842
298	−152.796	−22.264	39.727	−23.377
306	−150.376	−24.684	39.098	−25.918
310	−146.548	−28.512	38.102	−29.938

[a] All these values calculated according to the method of ref *35*.

rate constant values are nearly $(6.81 \pm 1.2) \times 10^3$ M^{-1} s^{-1} for the major fast phase and $(1.42 \pm 0.6) \times 10^3$ M^{-1} s^{-1} for the minor slow phase at 25 °C. This value is ∼10 times slower than that of AC binding to tubulin (*11*). The binding kinetics was also studied by monitoring the drug fluorescence. In this case, the drug fluorescence data were also resolved into two phases; the apparent second-order rate constant values are nearly 14.4×10^3 M^{-1} s^{-1} for the major fast phase and 1.39×10^3 M^{-1} s^{-1} for the minor slow phase. In both cases, the rate constant obtained in the slow phase is similar. However, the value of the fast phase is ∼2 times higher when measured using drug fluorescence. One of the possibilities for such differences could be due to the fact that both tubulin and indanocine concentrations are different in two experiments. For the drug-induced fluorescence, the concentrations of tubulin and indanocine used are 3 and 30 μM, respectively. Therefore, indanocine−tubulin binding follows the biphasic kinetics like the colchicine−tubulin interaction (*29, 30*). It is already known that colchicine can distinguish different tubulin isotypes and binds them with different affinities, which accounts for the origin of the biphasic kinetics observed in unfractionated tubulin (*31*−*33*). In an analogous manner, indanocine binding follows biphasic kinetics. Therefore, this drug can distinguish different isoforms of tubulin.

In this study, the thermodynamics of the indanocine−tubulin interaction was studied across a range of temperatures. It is evident from these experimental results that the reaction is enthalpy-driven with a large negative ΔC_p value of −175.1 cal mol^{-1} K^{-1}. The binding of drug to tubulin was mainly driven by a favorable change in ΔH. Thus, van der Waals interaction and hydrogen bonding might play a prominent role in the formation of the drug−tubulin complex as has been noted with several other protein−ligand interactions (*34*). The large ΔC_p value (−175.1 cal mol^{-1} K^{-1}) of indanocine−tubulin interaction confirms the establishment of a hydrophobic contact between the drug and protein interfaces. In addition, the enthalpically driven reaction suggests the presence of a hydrogen bonding interaction in the binding process.

A large negative value of ΔC_p is usually taken as an indicator of a dominant hydrophobic effect related to the binding process. For interpreting our data quantitatively, the empirical method of Sturtevant (*35*) was used to estimate the hydrophobic and intramolecular vibrational contribution to ΔC_p for indanocine (Table 3). As a result, the hydrophobic contribution to ΔC_p was found to be greater than the calculated vibrational contribution, corresponding to the prediction that the negative ΔC_p might originate from a favorable hydrophobic contribution. The hydrophobic effect generally brings two nonpolar surfaces closer together and depletes water from the binding surface, resulting in a positive change in ΔS. However, here we had the lowering of ΔS with an increase in temperature. Thus, there must be some other factors that overcome the hydrophobic effect, thereby making a smaller contribution to ΔS. The empirical method of Sturtevant (*35*) was again used to estimate the hydrophobic and intramolecular vibrational contribution to ΔS (Table 3). The sign of the calculated hydrophobic contribution to ΔS was positive, whereas that of the calculated vibrational contribution to ΔS was negative. With an increase in temperature, the vibrational contribution to entropy increased but the hydrophobic contribution remained more or less constant, thereby leading to the lowering of ΔS. The enthalpy-driven binding of indanocine to tubulin with an increase in temperature suggests that van der Waals interaction and hydrogen bonding between specific groups, together with an increased hydrophobic contribution, gave rise to such a negative value of ΔC_p.

Finally, from this study, one is curious to know how structurally dissimilar drugs recognize the same binding site. Ultimately, it is the pharmacophoric attachment points and interactions between different parts of the drugs and the amino acid residues of the binding site that determine the specificity of an interaction. While docking and molecular dynamics can give an idea of interactions using the crystal structure of the colchicine−tubulin complex as a template, the true picture of interactions requires the crystal structure of the tubulin−indanocine complex.

ACKNOWLEDGMENT

Prof. Gautam Basu of the Department of Biophysics, Bose Institute, is thankfully acknowledged for his suggestion. Pukhrambam Grihanjali Devi of the Saha Institute of Nuclear Physics is thankfully acknowledged for handling the stopped-flow fluorescence measurement.

REFERENCES

1. Avila, J. (1990) Microtubule dynamics. *FASEB J. 4*, 3284–3290.
2. Mollinedo, F., and Gajate, C. (2003) Microtubules, microtubule-interfering agents and apoptosis. *Apoptosis 8*, 413–450.
3. Sengupta, S., and Thomas, S. A. (2006) Drug target interaction of tubulin-binding drugs in cancer therapy. *Expert Rev. Anticancer Ther. 6*, 1433–1447.
4. Lee, K. H., Yim, E. K., Kim, C. J., Namkoong, S. E., Um, S. J., and Park, J. S. (2005) Proteomic analysis of anti-cancer effects by paclitaxel treatment in cervical cancer cells. *Gynecol. Oncol. 98*, 45–53.
5. Bacher, G., Nickel, B., Emig, P., Vanhoefer, U., Seeber, S., Shandra, A., Klenner, T., and Beckers, T. (2001) D-24851, a novel synthetic microtubule inhibitor, exerts curative antitumoral activity in vivo, shows efficacy toward multidrug-resistant tumor cells, and lacks neurotoxicity. *Cancer Res. 61*, 392–399.
6. Beckers, T., Reissmann, T., Schmidt, M., Burger, A. M., Fiebig, H. H., Vanhoefer, U., Pongratz, H., Hufsky, H., Hockemeyer, J., Frieser, M., and Mahboobi, S. (2002) 2-Aroylindoles, a novel class of potent, orally active small molecule tubulin inhibitors. *Cancer Res. 62*, 3113–3119.
7. Tahir, S. K., Nukkala, M. A., Zielinski Mozny, N. A., Credo, R. B., Warner, R. B., Li, Q., Woods, K. W., Claiborne, A., Gwaltney, S. L., Frost, D. J., Sham, H. L., Rosenberg, S. H., and Nq, S. C. (2003) Biological activity of A-289099: An orally active tubulin-binding indolyloxazoline derivative. *Mol. Cancer Ther. 2*, 227–233.
8. Kuo, C. C., Hsieh, H. P., Pan, W. Y., Chen, C. P., Liou, J. P., Lee, S. J., Chang, Y. L., Chen, L. T., Chen, C. T., and Chang, J. Y. (2004) BPR0L075, a novel synthetic indole compound with antimitotic activity in human cancer cells, exerts effective antitumoral activity in vivo. *Cancer Res. 64*, 4621–4628.

9. Aneja, R., Lopus, M., Zhou, J., Vangapandu, S. N., Ghaleb, A., Yao, J., Nettles, J. H., Zhou, B., Gupta, M., Panda, D., Chandra, R., and Joshi, H. C. (2006) Rational design of the microtubule-targeting anti-breast cancer drug EM015. *Cancer Res. 66*, 3782–3791.
10. Aneja, R., Zhou, J., Vangapandu, S. N., Zhou, B., Chandra, R., and Joshi, H. C. (2006) Drug-resistant T-lymphoid tumors undergo apoptosis selectively in response to an antimicrotubule agent, EM011. *Blood 107*, 2486–2492.
11. Leoni, L. M., Hamel, E., Genini, D., Shih, H., Carrera, C. J., Cottam, H. B., and Carson, D. A. (2000) Indanocine, a microtubule-binding indanone and a selective inducer of apoptosis in multidrug-resistant cancer cells. *J. Natl. Cancer Inst. 92*, 217–224.
12. Nguyen, T. L., McGrath, C., Hermone, A. R., Burnett, J. C., Zaharevitz, D. W., Day, B. W., Wipf, P., Hamel, E., and Gussio, R. (2005) *J. Med. Chem. 48*, 6107–6116.
13. Hamel, E., and Lin, C. (1981) Glutamate-induced polymerization of tubulin: Characteristics of the reaction and application to the large-scale purification of tubulin. *Arch. Biochem. Biophys. 209*, 29–40.
14. Lowry, O. H., Rosenbrough, N. J., Farr, A. I., and Randall, R. J. (1951) Protein measurement with the Folin phenol reagent. *J. Biol. Chem. 193*, 265–275.
15. Banerjee, A., and Luduena, R. F. (1987) Kinetics of association and dissociation of colchicine-tubulin complex from brain and renal tubulin. Evidence for the existence of multiple isotypes of tubulin in brain with differential affinity to colchicine. *FEBS Lett. 219*, 103–107.
16. Lakowicz, J. R. (1983) *Principles of Fluorescence Spectroscopy*, pp 1−44, Plenum Press, New York.
17. Pyles, E. A., and Hastie, S. B. (1993) Effect of the B ring and the C-7 substituent on the kinetics of colchicinoid-tubulin associations. *Biochemistry 32*, 2329–2336.
18. Bhattacharyya, B., and Wolff, J. (1974) Promotion of Fluorescence upon Binding of Colchicine to Tubulin. *Proc. Natl. Acad. Sci. U.S.A. 71*, 2627–2631.
19. Chattopadhyay, A., Rawat, S. S., Kelkar, D. A., Ray, S., and Chakrabarti, A. (2003) Organization and dynamics of tryptophan residues in erythroid spectrin: Novel structural features of denatured spectrin revealed by the wavelength-selective fluorescence approach. *Protein Sci. 12*, 2389–2403.
20. Ray, K., Bhattacharyya, B., and Biswas, B. B. (1981) Role of B-ring of colchicine in its binding to tubulin. *J. Biol. Chem. 256*, 6241–6244.
21. Bane, S., Puett, D., Macdonald, T. L., and Williams, R. C., Jr. (1984) Binding to tubulin of the colchicine analog 2-methoxy-5-(2′,3′,4′-trimethoxyphenyl) tropone. Thermodynamic and kinetic aspects. *J. Biol. Chem. 259*, 7391–7398.
22. Gupta, S., Das, L., Datta, A. B., Poddar, A., Janik, M. E., and Bhattacharyya, B. (2006) Oxalone and lactone moieties of podophyllotoxin exhibit properties of both the B and C rings of colchicine in its binding with tubulin. *Biochemistry 45*, 6467–6475.
23. Chakrabarti, G., Sengupta, S., and Bhattacharyya, B. (1996) Thermodynamics of colchicinoid-tubulin interactions. Role of B-ring and C-7 substituent. *J. Biol. Chem. 271*, 2897–2901.
24. Swaminathan, C. P., Nandi, A., Visweswariah, S. S., and Surolia, A. (1999) Thermodynamic Analyses Reveal Role of Water Release in Epitope Recognition by a Monoclonal Antibody against the Human Guanylyl Cyclase C Receptor. *J. Biol. Chem. 274*, 31272–31278.
25. Cleary, J., and Glick, G. D. (2003) Mutational analysis of a sequence-specific ssDNA binding lupus autoantibody. *Biochemistry 42*, 30–41.
26. Ortiz-Salmerón, E., Barón, C., and García-Fuentes, L. (1998) Enthalpy of captopril-angiotensin I-converting enzyme binding. *FEBS Lett. 435*, 219–224.
27. Ghisla, S., Massey, V., Lhoste, J. M., and Mayhew, S. G. (1974) Fluorescence and optical characteristics of reduced flavines and flavoproteins. *Biochemistry 13*, 589–597.
28. Tauscher, L., Ghisla, S., and Hemmerich, P. (1973) NMR study of nitrogen inversion and conformation of 1,5 dihydro-isoalloxazines ("reduced flavin"). Studies in the flavin series, XIX. *Helv. Chim. Acta 56*, 630–644.
29. Garland, D. L. (1978) Kinetics and mechanism of colchicine binding to tubulin: Evidence for ligand-induced conformational change. *Biochemistry 17*, 4266–4272.
30. Hadfield, J. A., Ducki, S., Hirst, N., and McGown, A. T. (2003) Tubulin and microtubules as targets for anticancer drugs. *Prog. Cell Cycle Res. 5*, 309–325.
31. Banerjee, A., and Luduena, R. F. (1992) Kinetics of colchicine binding to purified β-tubulin isotypes from bovine brain. *J. Biol. Chem. 267*, 13335–13339.
32. Banerjee, A., D'Hoore, A., and Engelborghs, Y. (1994) Interaction of desacetamidocolchicine, a fast binding analogue of colchicine with isotypically pure tubulin dimers $\alpha\beta$II, $\alpha\beta$III, and $\alpha\beta$IV. *J. Biol. Chem. 269*, 10324–10329.
33. Banerjee, A., Engelborghs, Y., D'Hoore, A., and Fitzgerald, T. J. (1997) Interactions of a bicyclic analog of colchicine with β-tubulin isoforms $\alpha\beta$(II), $\alpha\beta$(III) and $\alpha\beta$(IV). *Eur. J. Biochem. 246*, 420–424.
34. Torigoe, H., Nakayama, T., Imazato, M., Shimada, I., Arata, Y., and Sarai, A. (1995) The affinity maturation of anti-4-hydroxy-3-nitrophenylacetyl mouse monoclonal antibody. A calorimetric study of the antigen-antibody interaction. *J. Biol. Chem. 270*, 22218–22222.
35. Sturtevant, J. M. (1977) Heat capacity and entropy changes in processes involving proteins. *Proc. Natl. Acad. Sci. U.S.A. 74*, 2236–2240.

BI801575E